DOI: 10.19884/j.1672-5220.202405010

Morphology Control of TiO_2 Nanotubes towards High-Efficient Electrodes for Supercapacitor

WANG Jin, CHEN Guangbing, WANG Chunrui, LI Hui*
College of Physics, Donghua University, Shanghai 201620, China

Abstract: This article studies the role of electrochemical parameters in controlling the morphology of oxidized TiO_2 nanotubes and the electrochemical performance of modified TiO_2 nanotubes. Humidity is a key factor for fabricating TiO_2 nanotubes. When the relative humidity belows 70%, the TiO_2 nanotubes can be successfully prepared. What's more, by changing the anodization voltage and time, the diameter and the length of TiO_2 nanotubes can be adjusted. In addition, the TiO_2 nanotubes are modified through electrochemical self-doping and loading Pt metal particles on the surface of the nanotubes, which promotes the performance of the supercapacitor. The sample anodized at 100 V for 3 h has a specific capacity of up to 2.576 mF/cm^2 at a scan rate of 100 mV/s after self-doping, and its capacity retention rate still remains at 89.55% after 5 000 cycles, demonstrating excellent cycling stability. The Pt-modified sample has a specific capacity of up to 3.486 mF/cm^2 at the same scan rate, exhibiting more outstanding electrochemical performance.

Key words: TiO_2 nanotube; anodization; conductivity; supercapacitor
CLC number: O646 **Document code**: A
Article ID: 1672-5220(2024)04-0377-11

Open Science Identity (OSID)

0 Introduction

As an important type of an energy storage device[1], supercapacitor has become a research hotspot owing to its high power densities, fast charging speeds and long cycle life[2-6]. Supercapacitors can be categorized into electric double-layer capacitors (EDLCs) and pseudocapacitors based on the charge storage mechanisms. For EDLCs, electric charge is stored electrostatically at the interface between the active electrode and the electrolyte, with non-Faradic behavior. For pseudocapacitors, charge storage is via a reversible Faradic redox reaction[7]. Obtaining high-performance electrode materials is the key to the development of supercapacitors. TiO_2 is a semiconductor material with stable physical and chemical properties. Compared to other nanostructures, one-dimensional TiO_2 nanotubes have a larger specific surface area, a stronger adsorption capacity and a unique electron transport pathway. These advantages make them widely used in solar cells, photocatalysis, water splitting and supercapacitors[8-13]. Among the methods of manufacturing TiO_2 nanotubes, Ti foil anodization is an easy way to achieve self-organized TiO_2 nanotubes[14-15]. Therefore, anodized TiO_2 nanotubes have become a good choice for supercapacitor electrodes due to their stable electrochemical performance, good cycling performance, wide voltage window and low cost[16-18]. The self-assembling properties of TiO_2 nanotubes provide excellent templates for electrode active materials, enhancing their specific surface area and increasing the capacitance of supercapacitors. Additionally, the tubular structure of TiO_2 nanotubes serves as a fast pathway for electrolyte transportation, promoting efficient contact between electrode active materials and the electrolyte[5,19], and thus improving the capacitance of the electrode active materials under fast charging and discharging conditions.

Studies have shown that TiO_2 nanotubes with various morphology can be obtained by controlling anodization voltage, time, etc., and the microstructure and the conductivity of TiO_2 nanotubes play a crucial role in charge storage[9,20-21]. Berger et al.[22] anodized Ti foils at a voltage of 10, 20 and 40 V, respectively. Experimental results revealed that as the anodization voltage increased, the diameters of the TiO_2 nanotubes expanded, and the orderliness of the TiO_2 nanotubes also improved. Park et al.[23] conducted experiments in an NH_4F ethylene glycol solution with a mass fraction of 0.3% at a voltage of 60 V for 20, 30 and 40 min, resulting in nanotube lengths of 18.0, 25.2 and 30.8 μm, respectively. The diameter of the nanotubes remained around 40 nm in all cases. They concluded that with the increasing duration, the length of the nanotubes would gradually increase, while the diameter showed minimal variation. Ozkan et al.[24] anodized Ti foils at 30 V for 1 and 6 h in the dimethyl sulfoxide

Received date: 2024-05-16
Foundation item: National Natural Science Foundation of China (No. 12004070)
* Correspondence should be addressed to LI Hui, email: huili@dhu.edu.cn
Citation: WANG J, CHEN G B, WANG C R, et al. Morphology control of TiO_2 nanotubes towards high-efficient electrodes for supercapacitor [J]. *Journal of Donghua University (English Edition)*, 2024, 41(4): 377-387.

(DMSO) electrolyte, and fabricated 3 and 10 μm TiO_2 nanotubes, respectively. The 10 μm TiO_2 nanotubes exhibited a higher capacity than the 3 μm TiO_2 nanotubes apparently.

The conductivity of TiO_2 nanotubes can be improved partially through the above-mentioned morphological control. However, the capacitance value of the native TiO_2 nanotube supercapacitors is relatively low and cannot be commercialized due to the limitations of the native TiO_2. Specifically, the high electrical resistivity of native TiO_2 leads to a high internal resistance in TiO_2 nanotube supercapacitors. Therefore, modifying native TiO_2 has become an urgent problem to be solved. Introducing oxygen vacancies is a common method to modify native TiO_2. At present, the introduction of oxygen vacancies mainly relies on the methods including annealing treatment in a hydrogen atmosphere[18, 25], annealing treatment in an inert atmosphere (such as nitrogen and argon)[26-27], reducing solution treatment[28], hydrogen plasma treatment[29] and electrochemical self-doping under the cathode bias voltage[30]. Furthermore, metal element doping is also a common method of modifying native TiO_2. It uses physical or chemical ways to introduce highly conductive metal elements onto the surface of TiO_2 nanotubes, or introduce metal ions into the TiO_2 lattice, in order to introduce new charges, form defects, or change the lattice type in the lattice structure. The metal elements that have been extensively studied for modifying TiO_2 nanotubes include precious metals such as Ag, Au and Pt[31].

Few previous studies explored the influence of humidity on the preparation of TiO_2 nanotubes via anodization. Herein, we study the role of electrochemical parameters in controlling the morphology of oxidized TiO_2 nanotubes, including relative humidity, voltage and time. In addition, TiO_2 nanotubes are modified through electrochemical self-doping and Pt metal particle loading, which would promote the performance of the supercapacitor.

1 Materials and Methods

1.1 Synthesis of TiO_2 nanotubes

The Ti foils with a thickness of 0.2 mm and a purity higher than 99.5% (Baoji Ruicheng Co., Ltd., China) were ultrasonically cleaned in acetone, ethanol and deionized water for 30 min successively, and then dried in air before anodization. A mixed solution of 0.2 mol/L HF (Sigma-Aldrich, USA, a volume fraction of 48%) and 0.12 mol/L H_2O_2 (Sigma-Aldrich, a mass fraction of 3%) dissolved in ethylene glycol (Hushi, China, a volume fraction higher than 99.5%) was as the electrolyte. The electrolyte was aged for 12 h at 60 V before use. In a two-electrode electrochemical cell, with the Ti foil as the working anode and the Pt gauze as the counter electrode, electrochemical anodization was carried on the surface of the Ti foil and then TiO_2 nanotubes were attained. The Ti foil was pressed together with an Al foil against an O-ring, which defined a working area of 1.5 cm^2. Powered by Keithley 2400 Sourcemeter (USA), anodization happened at a constant voltage. A series of samples were obtained at 80 V for 2 h, 80 V for 3 h and 100 V for 3 h, respectively. The obtained TiO_2 sample was rinsed with deionized water and ethanol after anodization, and then dried in air. The as-anodized TiO_2 sample was annealed at 450 ℃ in air for 4 h at a heating rate of 3 ℃/min to crystallize amorphous TiO_2 into anatase TiO_2. This heat treatment was performed in a muffle furnace, and the sample placed inside an alumina crucible with an alumina cover to avoid contamination.

1.2 Electrochemical doping

As-annealed TiO_2 films first underwent an activation treatment (5 V for 30 min) in the mixed solution of 0.2 mol/L HF and 0.12 mol/L H_2O_2. Then a cathodic voltage (−2 V for 50 min) was adopted for the electrochemical self-doping process in a mixed solution of 0.5 mol/L Na_2SO_4 (Hushi, China, a mass fraction higher than 99.0%) and ethylene glycol (the volume ratio is 1∶1).

1.3 Pt loading

Samples were subjected to anodization at a voltage of 100 V for 3 h. Subsequently, after annealing and electrochemical self-doping, small-sized Pt metal particles were loaded onto the surface and the sidewalls of the samples. At room temperature, in a 10 mL beaker, 0.5 mmol/L chloroplatinic acid aqueous solution (5 mL) was added. Then, the as-doped TiO_2 nanotubes were placed into the beaker and stand in the dark for 4 h. Following this, the samples were rinsed with deionized water and ethanol to remove the residual chloroplatinic acid aqueous solution from the surface, and finally air-dried at room temperature.

1.4 Morphological and chemical characterization

Sample morphologies (top view and cross section) were observed by a field emission scanning electron microscope (FESEM, Hitachi, S-4800, Japan). X-ray diffraction (XRD) patterns of the samples were measured using a D/max-2550VB +/PC X-ray diffractometer (Rigaku, Japan, λ = 0.154 056 nm). The chemical composition of samples was characterized by an energy dispersive spectrometer (EDS) equipped with a JSM-7500F FESEM (JEOL, Japan).

1.5 Electrochemical measurements

Electrochemical measurements including cyclic voltammetry (CV) and galvanostatic charge/discharge (GCD) were achieved in a three-electrode electrochemical glass cell of 50 mL capacity by the electrochemical workstation (Shanghai Chenhua Instrument Co., Ltd., China) at room temperature. The sample was used as the working electrode. The counter

electrode and the reference electrode used a pure Pt foil (2 cm × 2 cm) and a saturated calomel reference electrode (SCE), respectively. Na_2SO_4 solution (0.5 mol/L) was used as the supporting electrolyte. CV was tested from 0 to 0.8 V at different scan rates (5, 20, 50 and 100 mV/s). GCD was tested at a current density of 50, 100, 150 and 200 μA/cm^2. The cycling stability of the supercapacitors was tested by using continuous CV cycling at a scan rate of 100 mV/s for 5000 cycles.

2 Results and Discussion

2.1 Influence of relative humidity on morphology of TiO_2 nanotubes

The influence of relative humidity on the morphology of TiO_2 nanotubes was studied. Relative humidity mainly regulates the morphology by affecting the effective current during the anodic oxidation process. Generally, the effective current is primarily determined by the applied voltage or current[32]. It is found that when the relative humidity is high enough, a large number of bubbles are generated in the electrolyte, indicating that the effective current increases significantly. When the relative humidity is approximately 50%, the current stabilizes at around 1 mA after 2 h anodic oxidation. As the relative humidity increases, the current gradually rises. When the relative humidity reaches 75%, the current approaches 2 mA. Numerous experiments reveal that when the relative humidity is maintained below 70%, samples with an area of 1.5 cm^2 can be successfully prepared, and these samples exhibit a uniform light yellow color and smooth surface, as shown in Fig. 1(a). However, when the relative humidity exceeds 70% during the anodic oxidation process, the large number of bubbles caused by the high current may potentially damage the already formed TiO_2 nanotubes. For instance, at room temperature and a constant voltage of 80 V, numerous small depressions initially appear on the surface of the formed nanotubes. As the reaction time increases, these depressions rupture and some parts of the TiO_2 film ultimately fall off, exposing the Ti substrate underneath (Fig. 1(b)). Based on the observed effects of humidity on anodic oxidation, a moderate relative humidity (≤50%) environment was maintained for all subsequent experimental procedures.

(a) (b)

Fig. 1 Optical photos of TiO_2 film obtained at relative humidity: (a) 50%; (b) 75%

2.2 Morphologic analysis

Figure 2 displays FESEM images of TiO_2 nanotubes prepared via constant-voltage anodization in the ethylene glycol electrolyte at room temperature. It is observed that the nanotubes are densely packed with uniformly sized nanopores and smooth tube walls. These nanotubes grow in a closely packed arrangement, exhibiting self-organization and controllable tubular structures.

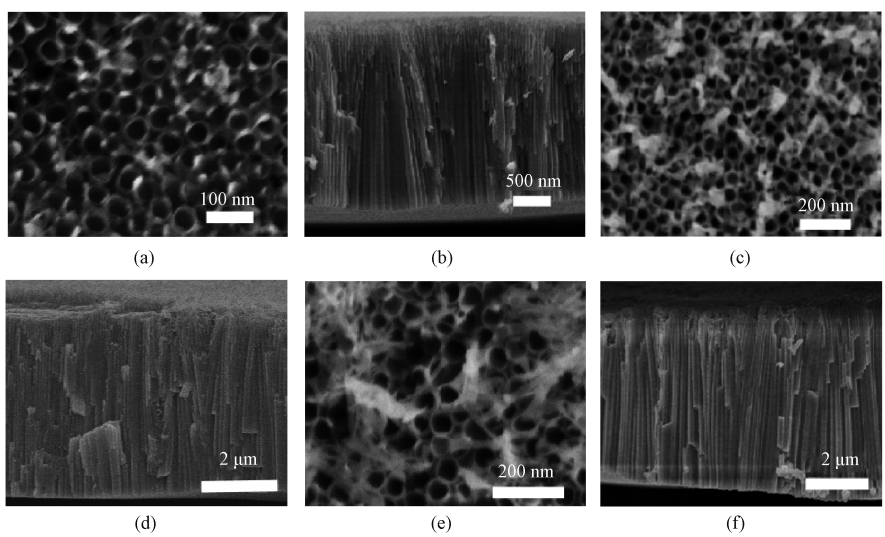

Fig. 2 FESEM images of TiO_2 nanotubes: (a)–(b) 80 V for 2 h; (c)–(d) 80 V for 3 h; (e)–(f) 100 V for 3 h

After 2 h anodization at a constant voltage of 80 V, the resulting nanotubes exhibit relatively thin and smooth tube walls with a diameter of 40 nm and a length of approximately 2.5 μm. When the anodization time increases to 3 h, the length of the prepared nanotubes increases to 5.0 μm (Fig. 2(d)), while the diameter is around 43 nm (Fig. 2(c)). Remarkably, during the additional hour of anodization, the diameter of the

nanotubes remains relatively unchanged, but the length of the nanotubes increases by 2.5 μm which is nearly equivalent to the length grown during the previous two hours. This indicates that the growth rate during the third hour is twice as fast as that during the first two hours. Previous studies have shown that the diameter of nanotubes is primarily determined by the anodization voltage, while the length is determined by the growth rate[22-23]. During the initial stage of anodization, a dense oxide film is first formed on the Ti substrate. As the anodization time increases, nanopores emerge on the surface of the oxide film, further forming regularly hexagonal-distributed nanotubes. Therefore, the initial stage of nanotube formation proceeds slowly, and as the formation and the etching of the TiO_2 film reach equilibrium, a stable growth rate is achieved[33-34]. This explains why the growth rate during the first two hours is only half of that in the third hour. Subsequent experimental results are also consistent with previous research findings. Figures 2(e) and 2(f) present the top view and the cross section of TiO_2 nanotubes prepared by anodization for 3 h at a voltage of 100 V, revealing that the nanotube diameter approaches 60 nm and the length reaches approximately 6.2 μm. Compared to Figs. 2(c) and 2(d), it is evident that both the diameter and the length of TiO_2 nanotubes can be adjusted by the voltage and the anodization time.

2.3 Electrochemical self-doping analysis

Figure 3 depicts the XRD spectra of as-anodized TiO_2 nanotubes, as-annealed TiO_2 nanotubes and as-doped TiO_2 nanotubes. The results indicate that the XRD spectrum of the as-annealed TiO_2 nanotubes exhibits typical characteristic peaks of anatase TiO_2, appearing at positions 25.5° (101), 37.9° (004), 47.8° (200), 54.0° (105) and 55.0° (211). The XRD spectrum of as-anodized TiO_2 nanotubes only shows characteristic peaks of the Ti substrate, indicating that the non-annealed TiO_2 nanotubes are amorphous. Therefore, the annealing process at 450 ℃ enables the transformation of TiO_2 from an amorphous state to a crystalline anatase phase[35].

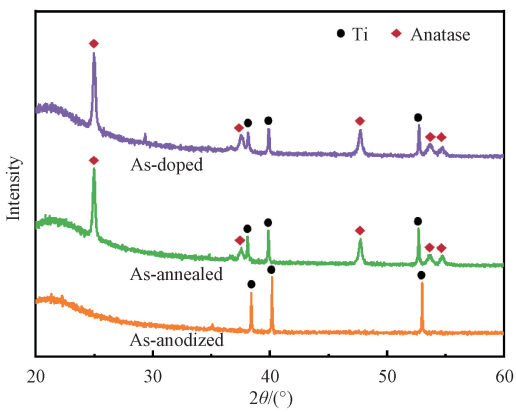

Fig. 3 XRD spectra of as-anodized, as-annealed and as-doped TiO_2 nanotubes

The influence of different crystal structure types on self-doping was also studied. Freshly prepared TiO_2 nanotubes from anodization are amorphous. When the resulted nanotubes were directly subjected to cathodic bias self-doping, the originally light-yellow TiO_2 film gradually turns black. However, upon removal of the voltage, the black color fades completely within a few minutes. Therefore, in this study, thermal treatment in air at 450 ℃ was conducted on the as-anodized TiO_2 nanotubes, transforming the amorphous TiO_2 into a more stable anatase phase, and the TiO_2 film turned deep blue, as depicted in Figs. 4(a) and 4(b). When the crystalline TiO_2 obtained after annealing was subjected to electrochemical cathodic doping, its color deepened further, as shown in Fig. 4(c), ultimately resulting in stable black TiO_2. In addition, the XRD spectrum reveals that the as-doped TiO_2 nanotubes still maintain the anatase crystal phase (Fig. 3).

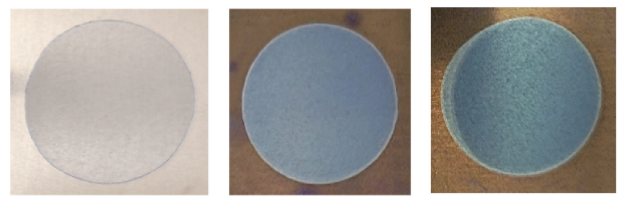

Fig. 4 Optical photos: (a) as-anodized TiO_2 film; (b) as-annealed TiO_2 film; (c) as-doped TiO_2 film

2.4 Electrochemical analysis

Figure 5 illustrates the electrochemical performance of samples through anodization. All the samples were followed by annealing at 450 ℃ in air and subsequent electrochemical cathodic self-doping treatment. According to the different anodization conditions of 80 V for 2 h, 80 V for 3 h and 100 V for 3 h, they were labeled as samples A1, A2 and A3, respectively. Figure 5(a) presents the CV curves of the three samples at a scan rate of 100 mV/s. It can be seen that all the curves are approximately rectangular, which indicates that there are only a few Faradaic reactions occurring within the studied potential window for all the samples. This suggests that the capacitors act dominated by EDLC[36].

As for the area enclosed by the curves, sample A1 has the smallest area, while sample A3 has the largest area, indicating that sample A3 has the best capacitance performance as a supercapacitor electrode. Therefore, increasing the anodization time at the same voltage or increasing the anodization voltage within the same time frame can improve the electrochemical performance of TiO_2 nanotubes. This is further confirmed by Figs. 5(b)–5(d). The GCD curves (Fig. 5(b)) exhibit excellent symmetry, indicating their outstanding reversibility. In a specific voltage range and at a discharge current density, the smoother the discharge curve of a sample is, the

longer it takes to complete the discharge, indicating that the sample has a larger capacitance value[37]. Sample A3 exhibits the longest discharge time which reveals its best electrochemical performance. Figure 5(c) demonstrates the specific capacitance characteristics of each sample at different scan rates. As the scan rate increases from 5 mV/s to 100 mV/s, the area-specific capacitances of samples A1, A2 and A3 decrease by 16.6%, 11.1% and 16.3%, respectively, showing good rate performance. Figure 5(d) shows the CV cycle stability at a scan rate of 100 mV/s. After 5 000 cycles, the capacity retention rates of samples A1, A2 and A3 are 87.35%, 68.92% and 89.55%, respectively. The differences in electrochemical performance among these three samples are attributed to their differences in the microstructure. Sample A1 has the shortest nanotube length of about 2.5 μm, while sample A3 has a relatively large specific surface area and active material mass due to its longest nanotube length of 6.2 μm. Energy storage in double-layer capacitors is achieved through charge separation and accumulation at the electrode-electrolyte interface, and the capacitance is proportional to the electrode area and the mass of the active material. Therefore, increasing the specific surface area of TiO_2 nanotubes is an effective way to enhance the performance of double-layer capacitors.

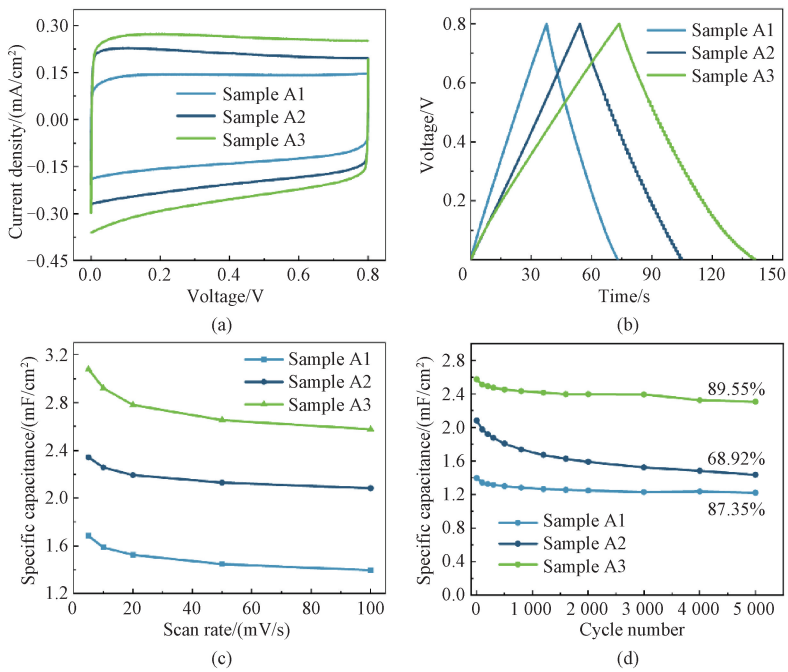

Fig. 5 Electrochemical performance of samples A1, A2 and A3: (a) CV curves at a scan rate of 100 mV/s; (b) GCD curves at current density of 50 μA/cm²; (c) specific capacitance; (d) CV cycle performance at a scan rate of 100 mV/s

In order to further test the influence of metal heteroatoms on electrochemical performance, the as-anodized TiO_2 nanotubes by 100 V for 3 h were selected and subjected to sequential thermal annealing, self-doping and loading small-sized Pt particles on the surface to form a heterojunction structure. The performance of different samples was compared. The preparation parameters of different samples are listed in Table 1 and the samples are labeled as samples B1, B2 and B3.

Table 1 Sample preparation parameters

Sample	As-anodized	As-annealed	Activation	As-doped	Pt-loaded
B1	100 V, 3 h	450 ℃, 4 h	—	—	—
B2	100 V, 3 h	450 ℃, 4 h	5 V, 30 min	−2 V, 50 min	—
B3	100 V, 3 h	450 ℃, 4 h	5 V, 30 min	−2 V, 50 min	Stand for 4 h

Figures 6 and 7 show the surface scanning EDS spectra of samples B1 and B3, respectively. It can be observed that the elemental mappings of both samples exhibit uniform distributions of O and Ti elements. However, a small amount of uniformly distributed Pt is detected on the surface of sample B3. As evident from the enlarged inset in Fig. 7(d), the mass fraction of the loaded Pt accounts for approximately 0.37%.

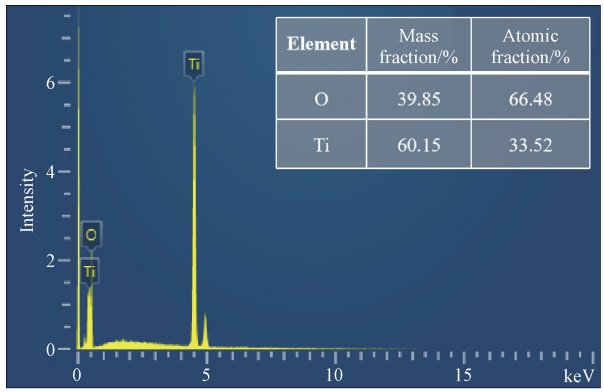

Fig. 6 EDS results of sample B1: (a) total element distribution; (b) EDS mapping of Ti; (c) EDS mapping of O

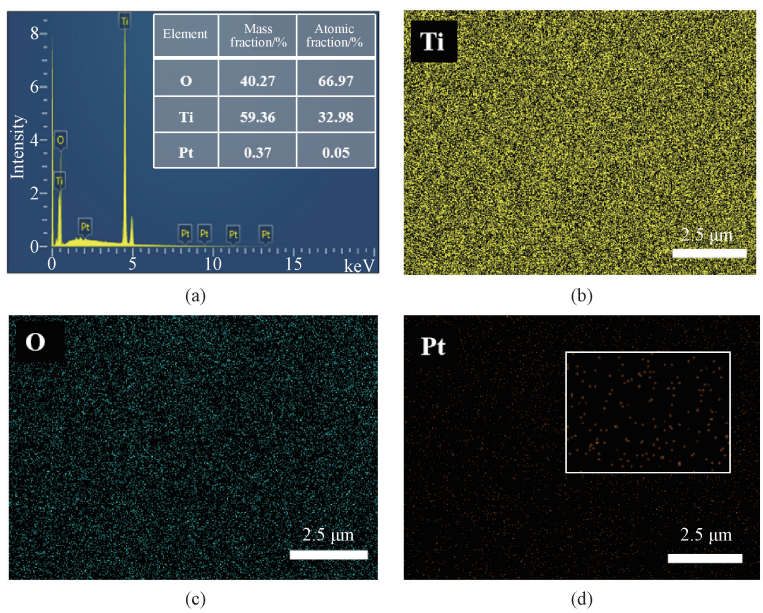

Fig. 7 EDS results of sample B3: (a) total element distribution; (b) EDS mapping of Ti; (c) EDS mapping of O; (d) EDS mapping of Pt

TiO_2 nanotubes of samples B1, B2 and B3 were employed as electrode materials for supercapacitors, and their electrochemical performances were investigated. Figure 8 (a) presents the CV curves for the three samples at a scan rate of 100 mV/s. All curves exhibit nearly rectangular shapes, indicating the behavior of EDLC dominating within the studied potential window. Additionally, sample B1 displays the smallest enclosed area in the CV curve, suggesting the minimal capacity and the poorest capacitive performance. In contrast, the enclosed area of the CV curve of sample B2 is noticeably larger than that of sample B1, indicating that electrochemical cathodic self-doping treatment effectively enhances the capacitive performance of TiO_2 nanotubes. The enhancement in capacitance could be attributed to the significant decrease in charge-transport resistance, which is accomplished by introducing oxygen vacancy sites through electrochemical cathodic self-

doping treatment[38]. Researches have shown that hydrogenation of TiO_2 nanotubes leads to an increase in the density of hydroxyl groups on the TiO_2 nanotube surface, thereby enhancing its specific capacitance[18]. Furthermore, the electrochemical cathodic self-doping process of TiO_2 nanotubes forms pathways for the insertion/deinsertion of H^+ ions, which may facilitate the insertion/deinsertion of H^+ and Na^+ ions when TiO_2 nanotubes are used as active materials in supercapacitors[38].

Moreover, loading Pt onto the as-doped TiO_2 nanotubes further enhances the capacity of TiO_2 nanotubes as electrodes for supercapacitors, which is demonstrated by the largest enclosed area of the CV curve of sample B3, as shown in Fig. 8(a). At a scan rate of 100 mV/s, the specific capacitance of sample B1 is only 0.230 mF/cm^2, while that of sample B2 reaches 2.576 mF/cm^2, and the specific capacitance of sample B3 increases to 3.486 mF/cm^2.

Figure 8(b) exhibits the GCD curves of samples B1, B2 and B3 at a current density of 50 μA/cm^2. During charging and discharging processes, all three samples display linear voltage changes and good symmetry, indicating their excellent double-layer capacitance characteristics. The results are consistent with the performance features reflected in the CV curves in Fig. 8(a). Sample B3 clearly exhibits a longer discharge time, indicating a larger capacitance value. Figure 8(c) demonstrates the variation of specific capacitance with the scan rate. It can be observed that the specific capacitance of samples B1, B2 and B3 remains stable as the scan rate increases. Specifically, as the scan rate increases from 5 mV/s to 100 mV/s, the specific capacitance of sample B3 retains 73.5%, demonstrating its excellent rate capability. Furthermore, Fig. 8(d) shows the GCD measurement results for sample B3. At a charge-discharge current density of 50 μA/cm^2, the specific capacitance is calculated to be 5.812 mF/cm^2. When the charge-discharge current density increases to 100 μA/cm^2, the specific capacitance is 3.725 mF/cm^2, and it decreases slightly to 3.424 mF/cm^2 when the charge-discharge current density increases to 200 μA/cm^2, further proving the excellent rate performance of Pt-loaded TiO_2 nanotubes.

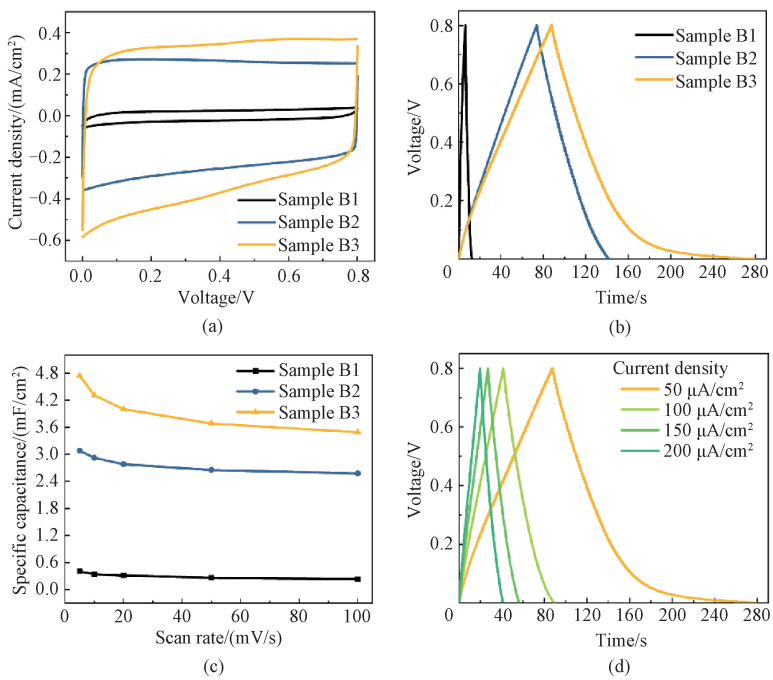

Fig. 8 Electrochemical performance of samples B1, B2 and B3: (a) CV curves at a scan rate of 100 mV/s; (b) GCD curves at a current density of 50 μA/cm^2; (c) specific capacitance; (d) GCD curves of sample B3 at different charge-discharge current densities of 50, 100, 150 and 200 μA/cm^2

The charge storage mechanism is regulated by both diffusion and surface capacitive processes. The Trasatti's method offers a quantitative approach to discern contributions of diffusion-controlled effects and surface-controlled effects, respectively[39]. The total capacitance C_T is delineated as the sum of diffusion-controlled capacitance C_i and surface-controlled capacitance C_o:

$$C_T = C_i + C_o. \quad (1)$$

The pseudocapacitance (PC) characterizes the diffusion-controlled capacitance, stemming from charge transfer within the bulk materials through insertion/extraction processes. While the surface-controlled capacitance, identified as capacitance of EDLC, occurs on the surface of materials. The specific capacitance

$C(v)$ as a function of the scan rate v is proportional to $v^{-1/2}$, assuming the semi-infinite linear diffusion[40-41]:

$$C(v) = kv^{-1/2} + C_0, \quad (2)$$

where k and C_0 are constants. The diffusion into bulk materials becomes more unfeasible at higher scan rates, therefore the capacitance equals C_0 when the scan rate approaches infinity ($v \rightarrow \infty$). Consequently, the C-intercept of the plot between $C(v)$ and $v^{-1/2}$ can be regarded as C_0. As shown in Fig. 9 (a), the C-intercept of the fitted linear is 2.445 and 3.165 for samples B2 and B3, respectively. Accordingly, the EDLC capacitance values are obtained. Further, the capacitance ratio of EDLC capacitance to PC can be obtained based on Eq. (2). As shown in Figs. 9 (b)–9(c), as the scan rate increases, the proportion of EDLC capacitance gradually increases. Compared to sample B2, sample B3 exhibits a higher PC proportion, indicating that the doping of Pt enhances the Faradaic redox reactions within the bulk TiO_2 nanotubes. When the scan rate increases from 5 to 100 mV/s, the PC proportion of sample B2 decreases from 20.6% to 5.1%, and for sample B3, the PC proportion decreases from 33.3% to 9.2%. This is because that as the scan rate increases, the efficiency of ion insertion into the interior of the electrode material is affected, thus impacting the efficiency of the redox reaction.

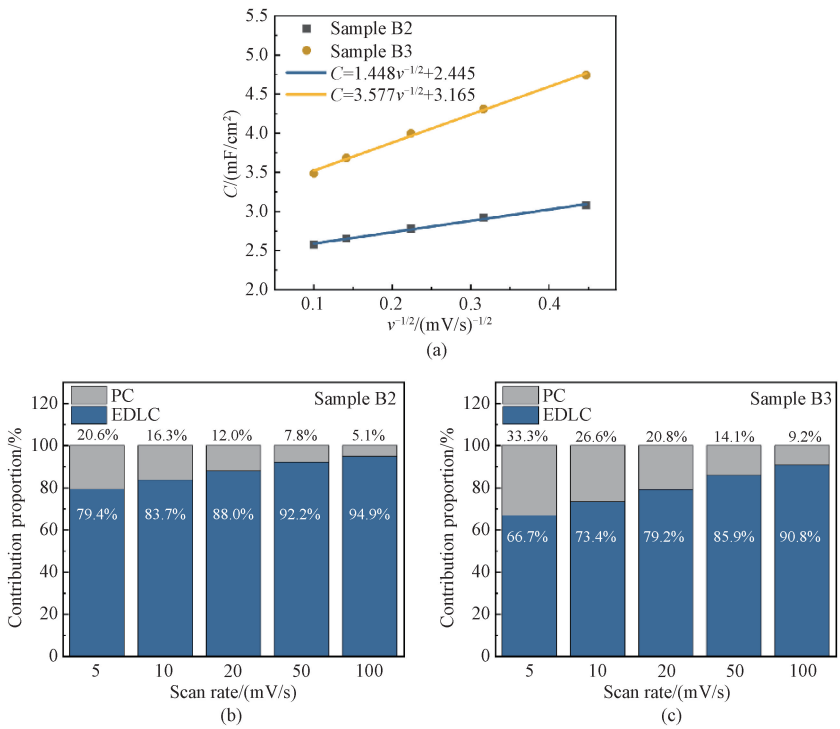

Fig. 9 Capacitance analysis: (a) correlation of C vs $v^{-1/2}$; (b) contribution proportion for sample B2; (c) contribution proportion for sample B3

The enhanced performance of TiO_2 nanotube electrodes after Pt loading can be elucidated utilizing the band theory. The bandgap of anatase TiO_2 is 3.2 eV, with a work function of 4.2 eV[42], while Pt possesses a work function of 5.65 eV. The work functions of both the semiconductor and the metal are crucial for the resulting state upon their contact. As illustrated in Fig. 10, the band alignment between anatase TiO_2 and Pt depicts that the work function of TiO_2 is lower than that of Pt. Upon contact, a Schottky barrier is formed at the interface between TiO_2 and Pt. Pt-loaded TiO_2 nanotubes are employed as electrodes in supercapacitors. During charging and discharging processes of the capacitor, a significant number of electrons can either pass through the Schottky barrier or overcome the built-in barrier, facilitating the transport throughout the entire composite material of Pt-loaded TiO_2 nanotubes under the influence of the electric field. The Schottky junction formed at the Pt-TiO_2 interface enhances the conductivity of TiO_2 nanotubes, thereby significantly improving their electrochemical performance as electrodes in supercapacitors. This effectively proves that electrodes with heterogeneous atom doping can improve their charge storage capacity[43].

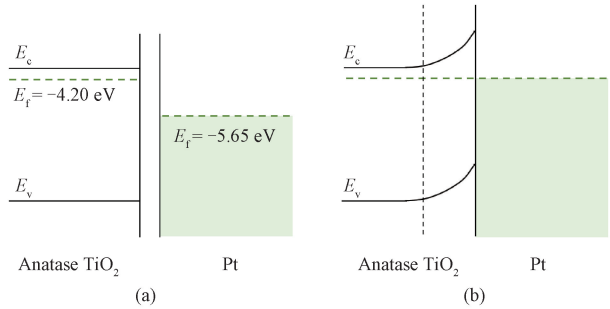

E_c—conduction band; E_v—valence band; E_f—Fermi level.

Fig. 10 Energy-band diagrams of anatase TiO_2 and Pt: (a) before contact; (b) after contact

3 Conclusions

In summary, a study of TiO_2 nanotubes via anodization at different voltages and time was carried out to explore the effect of anodization voltage and time on the morphology of TiO_2 nanotubes, as well as the electrochemical performance of TiO_2 nanotubes with different diameters and lengths prepared at 80 V for 2 h, 80 V for 3 h and 100 V for 3 h. Electrochemical self-doping was conducted on the anatase TiO_2 nanotubes, which significantly improved the electrochemical performance of TiO_2 nanotubes as the electrode for supercapacitors. With all doped samples being applied to the supercapacitor, the sample prepared at 100 V for 3 h showed the maximal capacitance. Additionally, Pt-loading further enhanced capacity of TiO_2 nanotubes for supercapacitors.

References

[1] SIMON P, GOGOTSI Y. Materials for electrochemical capacitors [J]. *Nature Materials*, 2008, 7(11): 845-854.

[2] ZHANG S L, PAN N. Supercapacitors performance evaluation [J]. *Advanced Energy Materials*, 2015, 5(6): 1401401.

[3] XIANG R F, CHEN X Y, LIU Y, et al. Porous graphene-based electrodes for fiber-shaped supercapacitors with good electrical conductivity [J]. *Journal of Donghua University (English Edition)*, 2023, 40(2): 134-141.

[4] QIAN Y C, YANG X X, ZHANG J J, et al. Research progress in electrode materials for supercapacitor [J]. *Journal of Donghua University (Natural Edition)*, 2022, 48(6): 1-13. (in Chinese)

[5] RAJ C C, PRASANTH R. Review: advent of TiO_2 nanotubes as supercapacitor electrode [J]. *Journal of the Electrochemical Society*, 2018, 165(9): E345.

[6] BORENSTEIN A, HANNA O, ATTIAS R, et al. Carbon-based composite materials for supercapacitor electrodes: a review [J]. *Journal of Materials Chemistry A*, 2017, 5(25): 12653-12672.

[7] SALARI M, ABOUTALEBI S H, KONSTANTINOV K, et al. A highly ordered titania nanotube array as a supercapacitor electrode [J]. *Physical Chemistry Chemical Physics: PCCP*, 2011, 13(11): 5038-5041.

[8] LIU S H, WANG Z Y, YU C, et al. A flexible TiO_2(B)-based battery electrode with superior power rate and ultralong cycle life [J]. *Advanced Materials*, 2013, 25(25): 3462-3467.

[9] GHICOV A, SCHMUKI P. Self-ordering electrochemistry: a review on growth and functionality of TiO_2 nanotubes and other self-aligned MO_x structures [J]. *Chemical Communications*, 2009, 28(20): 2791-2808.

[10] CHEN J S, CHEN C P, LIU J, et al. Ellipsoidal hollow nanostructures assembled from anatase TiO_2 nanosheets as a magnetically separable photocatalyst [J]. *Chemical Communications*, 2011, 47(9): 2631-2633.

[11] YE M D, LIU H Y, LIN C J, et al. Hierarchical rutile TiO_2 flower cluster-based high efficiency dye-sensitized solar cells via direct hydrothermal growth on conducting substrates [J]. *Small*, 2013, 9(2): 312-321.

[12] YANG P Y, ZHOU X Y, CAO G Z, et al. P3HT: PCBM polymer solar cells with TiO_2 nanotube aggregates in the active layer [J]. *Journal of Materials Chemistry*, 2010, 20(13): 2612-2616.

[13] FUJISHIMA A, HONDA K. Electrochemical photolysis of water at a semiconductor electrode [J]. *Nature*, 1972, 238(5358): 37-38.

[14] SO S, HWANG I, SCHMUKI P. Hierarchical DSSC structures based on "single walled" TiO_2 nanotube arrays reach a back-side illumination solar light conversion efficiency of 8% [J]. *Energy & Environmental Science*, 2015, 8(3): 849-854.

[15] GUI Q F, YU D L, LI D D, et al. Efficient suppression of nanograss during porous anodic

TiO_2 nanotubes growth [J]. *Applied Surface Science*, 2014, 314(1): 505-509.
[16] ZHOU H, ZHANG Y R. Electrochemically self-doped TiO_2 nanotube arrays for supercapacitors [J]. *The Journal of Physical Chemistry C*, 2014, 118(11): 5626-5636.
[17] LAMBERTI A, PIRRI C F. TiO_2 nanotube array as biocompatible electrode in view of implantable supercapacitors[J]. *Journal of Energy Storage*, 2016, 8(1): 193-197.
[18] LU X H, WANG G M, ZHAI T, et al. Hydrogenated TiO_2 nanotube arrays for supercapacitors[J]. *Nano Letters*, 2012, 12(3): 1690-1696.
[19] ANITHA V C, BANERJEE A N, DILLIP G R, et al. Nonstoichiometry-induced enhancement of electrochemical capacitance in anodic TiO_2 nanotubes with controlled pore diameter [J]. *Journal of Physical Chemistry C*, 2016, 120 (18): 9569-9580.
[20] MACAK J M, SCHMUKI P. Anodic growth of self-organized anodic TiO_2 nanotubes in viscous electrolytes[J]. *Electrochimica Acta*, 2006, 52 (3): 1258-1264.
[21] YORIYA S, PAULOSE M, VARGHESE O K, et al. Fabrication of vertically oriented TiO_2 nanotube arrays using dimethyl sulfoxide electrolytes [J]. *The Journal of Physical Chemistry C*, 2007, 111(37): 13770-13776.
[22] BERGER S, TSUCHIYA H, SCHMUKI P. Transition from nanopores to nanotubes: self-ordered anodic oxide structures on titanium-aluminides[J]. *Chemistry of Materials*, 2008, 20(10): 3245-3247.
[23] PARK H, KIM H G, CHOI W Y. Characterizations of highly ordered TiO_2 nanotube arrays obtained by anodic oxidation [J]. *Transactions on Electrical Electronic Materials*, 2010, 11(3): 112-115.
[24] OZKAN S, VALLE F, MAZARE A, et al. Optimized polymer electrolyte membrane fuel cell electrode using TiO_2 nanotube arrays with well-defined spacing [J]. *ACS Applied Nano Materials*, 2020, 3(5): 4157-4170.
[25] ZHU S S, ZHANG P P, CHANG L, et al. Photochemical fabrication of 3D hierarchical Mn_3O_4/H-TiO_2 composite films with excellent electrochemical capacitance performance [J]. *Physical Chemistry Chemical Physics*, 2016, 18 (12): 8529-8536.
[26] SALARI M, KONSTANTINOV K, LIU H K. Enhancement of the capacitance in TiO_2 nanotubes through controlled introduction of oxygen vacancies [J]. *Journal of Materials Chemistry*, 2011, 21(13): 5128-5133.
[27] PEI Z X, ZHU M S, HUANG Y, et al. Dramatically improved energy conversion and storage efficiencies by simultaneously enhancing charge transfer and creating active sites in MnO_x/TiO_2 nanotube composite electrodes[J]. *Nano Energy*, 2016, 20(1): 254-263.
[28] ZHANG J F, WANG Y, WU J J, et al. Remarkable supercapacitive performance of TiO_2 nanotube arrays by introduction of oxygen vacancies [J]. *Chemical Engineering Journal*, 2017, 313(1): 1071-1081.
[29] WU H, XU C, XU J, et al. Enhanced supercapacitance in anodic TiO_2 nanotube films by hydrogen plasma treatment [J]. *Nanotechnology*, 2013, 24(45): 455401.
[30] KIM C, KIM S, HONG S P, et al. Effect of doping level of colored TiO_2 nanotube arrays fabricated by electrochemical self-doping on electrochemical properties [J]. *Physical Chemistry Chemical Physics*, 2016, 18 (21): 14370-14375.
[31] MOHAMED A E R, ROHANI S. Modified TiO_2 nanotube arrays (TNTAs): progressive strategies towards visible light responsive photoanode, a review [J]. *Energy & Environmental Science*, 2011, 4(4): 1065-1086.
[32] CHONG B, YU D L, JIN R, et al. Theoretical derivation of anodizing current and comparison between fitted curves and measured curves under different conditions[J]. *Nanotechnology*, 2015, 26(14): 145603.
[33] SU Z X, ZHOU W Z. Formation mechanism of porous anodic aluminium and titanium oxides [J]. *Advanced Materials*, 2008, 20(19): 3663-3667.
[34] REGONINI D, BOWEN C R, JAROENWORALUCK A, et al. A review of growth mechanism, structure and crystallinity of anodized TiO_2 nanotubes[J]. *Materials Science and Engineering: R: Reports*, 2013, 74(12): 377-406.
[35] ALBU S P, TSUCHIYA H, FUJIMOTO S, et al. TiO_2 nanotubes-annealing effects on detailed morphology and structure[J]. *European Journal of Inorganic Chemistry*, 2010, 2010 (27): 4351-4356.
[36] LEE D Y, JUNG J Y, JUNG M J, et al. Hierarchical porous carbon fibers prepared using a SiO_2 template for high-performance EDLCs[J]. *Chemical Engineering Journal*, 2015, 263(1): 62-70.
[37] ZHANG Y L, LI X, LI Z H, et al. Evaluation of electrochemical performance of supercapacitors from equivalent circuits through cyclic voltammetry and galvanostatic charge/discharge [J]. *Journal of Energy Storage*, 2024, 86(1): 111122.

[38] LI H, CHEN Z H, TSANG C K, et al. Electrochemical doping of anatase TiO_2 in organic electrolytes for high-performance supercapacitors and photocatalysts [J]. *Journal of Materials Chemistry A*, 2014, 2(1): 229-236.
[39] SHAO J J, ZHOU X Y, LIU Q, et al. Mechanism analysis of the capacitance contributions and ultralong cycling-stability of the isomorphous MnO_2 @ MnO_2 core/shell nanostructures for supercapacitors[J]. *Journal of Materials Chemistry A*, 2015, 3(11): 6168-7176.
[40] SIM C K, MAJID S R, MAHMOOD N Z. $ZnSnO_3$/mesoporous biocarbon composite towards sustainable electrode material for energy storage device [J]. *Microchemical Journal*, 2021, 164(1): 105968.
[41] PHOLAUYPHON W, BULAKHE R N, PRANEERAD J, et al. Ultrahigh-performance titanium dioxide-based supercapacitors using sodium polyacrylate-derived carbon dots as simultaneous and synergistic electrode/electrolyte additives[J]. *Electrochimica Acta*, 2021, 390(1): 138805.
[42] SWAMINATHAN J, RAVICHANDRAN S. Insights into the electrocatalytic behavior of defect-centered reduced titania ($TiO_{1.23}$) [J]. *The Journal of Physical Chemistry C*, 2018, 122(3): 1670-1680.
[43] HUANG Z H, LIU T Y, SONG Y, et al. Balancing the electrical double layer capacitance and pseudocapacitance of hetero-atom doped carbon[J]. *Nanoscale*, 2017, 9(35): 13119-13127.

优化 TiO_2 纳米管形貌以构建高性能超级电容器电极

王 瑾, 陈广冰, 王春瑞, 李 惠*
东华大学 物理学院, 上海 201620

摘 要: 该文研究了电化学参数对于阳极氧化 TiO_2 纳米管的形貌调控作用, 以及修饰改性对 TiO_2 纳米管电化学性能的影响。湿度是决定能否成功制备样品的关键因素, 当相对湿度低于 70%时, 可得到完好的 TiO_2 纳米管膜层。通过改变氧化电压和时间, 可调控 TiO_2 纳米管的管径和管长。此外, 通过电化学自掺杂和在纳米管的表面负载 Pt 金属颗粒对 TiO_2 纳米管进行修饰, 提升了超级电容器的性能。对于经自掺杂 100 V 电压氧化 3 h 的样品, 在 100 mV/s 的扫描速率下, 其比容量达到 2.576 mF/cm^2, 经过 5000 次循环, 其容量保持率仍达到 89.55%, 呈现优异的倍率性能。经 Pt 修饰的样品, 在相同的扫描速率下, 其比容量高达 3.486 mF/cm^2, 展现出更为出色的电化学性能。

关键词: TiO_2 纳米管; 阳极氧化; 导电性; 超级电容器